THE JOURNAL OF BIOLOGICAL CHEMISTRY VOL. 282, NO. 16, pp. 12143–12153, April 20, 2007

Actin-binding Protein α-Actinin-1 Interacts with the Metabotropic Glutamate Receptor Type 5b and Modulates the Cell Surface Expression and Function of the Receptor*

Received for publication, September 15, 2006, and in revised form, February 7, 2007 Published, JBC Papers in Press, February 20, 2007, DOI 10.1074/jbc.M608880200

Nuria Cabello[‡], Rosaria Remelli[§1], Laia Canela[‡], Ana Soriguera[‡], Josefa Mallol[‡], Enric I. Canela[‡], Melanie J. Robbins[¶], Carme Lluis[‡], Rafael Franco[‡], R. A. Jeffrey McIlhinney[§], and Francisco Ciruela[‡2]

From the [‡]Institut d'Investigacions Biomèdiques August Pi i Sunyer and Department of Biochemistry and Molecular Biology, University of Barcelona, Facultat de Biologia, Avda. Diagonal 645, Barcelona 08028, Spain, the [§]Medical Research Council Anatomical Neuropharmacology Unit, Oxford OX1 3TH, United Kingdom, and the [¶]Department of Schizophrenia & Bipolar Neurophysiology and Pharmacology, Psychiatry Centre of Excellence for Drug Discovery, GlaxoSmithKline Pharmaceuticals, Harlow, Essex CM19 5AW, United Kingdom

Receptors for neurotransmitters require scaffolding proteins for membrane microdomain targeting and for regulating receptor function. Using a yeast two-hybrid screen, α-actinin-1, a major F-actin cross-linking protein, was identified as a binding partner for the C-terminal domain of metabotropic glutamate receptor type 5b ($mGlu_{5b}$ receptor). Co-expression, co-immunoprecipitation, and pull-down experiments showed a close and specific interaction between $mGlu_{5b}$ receptor and α-actinin-1 in both transfected HEK-293 cells and rat striatum. The interaction of α-actinin-1 with $mGlu_{5b}$ receptor modulated the cell surface expression of the receptor. This was dependent on the binding of α-actinin-1 to the actin cytoskeleton. In addition, the α-actinin-1/$mGlu_{5b}$ receptor interaction regulated receptor-mediated activation of the mitogen-activated protein kinase pathway. Together, these findings indicate that there is an α-actinin-1-dependent $mGlu_{5b}$ receptor association with the actin cytoskeleton modulating receptor cell surface expression and functioning.

Glutamate and aspartate are the major excitatory neurotransmitters in the mammalian central nervous system (1, 2). These excitatory amino acids act on glutamate receptors and play an important role in many physiological functions, including learning, memory, and development (3). Glutamate receptors are widely distributed in the central nervous system and include three subtypes of ionotropic glutamate receptors (α-amino-3-hydroxy-5-methyl-4-isoxazolepropionic acid, NMDA,[3] and kainate receptors) and a family of G protein-coupled metabotropic glutamate (mGlu) receptors that act through different second messenger pathways. Eight members of the mGlu receptor family have been identified and categorized into three subgroups on the basis of their sequence homology, agonist selectivity and signal transduction pathway. Group I contains the $mGlu_1$ and $mGlu_5$ receptor subtypes, which are coupled to phospholipase C in transfected cells and have quisqualic acid as their most potent agonist (4). The $mGlu_5$ receptor is expressed in two splice variants, $mGlu_{5a}$ and $mGlu_{5b}$, which differ in that $mGlu_{5b}$ has a 33-amino acid insert in the intracellular C-terminal domain. Interestingly, both subtypes of $mGlu_5$ are heavily expressed in striatum with the consideration that $mGlu_{5b}$ might be considered as an "adult" variant and $mGlu_{5a}$ is more a "neonatal" variant (5).

The actin-based cytoskeleton is connected to the plasma membrane via a lattice-like network of actin-binding proteins that form the membrane skeleton or membrane-associated cytoskeleton (6). The major structural component of the membrane skeleton is spectrin (also referred to as fodrin in non-erythroid cells), a flexible rod-shaped molecule composed of homologous, but non-identical α- and β-subunits. Other actin-binding proteins, like filamin A and α-actinin, also participate in the maintenance of this membrane-associated cytoskeleton and are essential for the anchoring of transmembrane proteins. A major F-actin cross-linking protein (7), present in both muscle and non-muscle cells, is α-actinin. There are four α-actinin genes, two non-skeletal muscle isoforms, α-actinin-1 and -4, and two skeletal muscle isoforms, α-actinin-2 and -3 (8). All of them share a general structure, which can be divided into three functionally distinct domains: the N terminus containing two calponin homology domains that bind to actin filaments (9), a central region composed of four spectrin-like motifs (10), which acts as a switchboard for interactions with multiple proteins, and the C terminus, which contains EF-hand domains responsible for Ca^{2+} binding (11) and terminates in a PDZ domain-binding sequence, ESDL (12) (for review see Refs. 13

* This work was supported by the Ministerio de Educación y Ciencia (Grant SAF2006-05481 to R. F., Grant SAF2005-00170 to E. C., and Grant SAF2005-00903 to F. C.). The costs of publication of this article were defrayed in part by the payment of page charges. This article must therefore be hereby marked "*advertisement*" in accordance with 18 U.S.C. Section 1734 solely to indicate this fact.

[1] A Ph.D. student funded by GlaxoSmithKline (UK) and the Biotechnology and Biological Sciences and Research Council.

[2] Recipient of a Ramón y Cajal research contract signed with the Ministerio de Educación y Ciencia. To whom correspondence should be addressed. Tel.: 34-934-039-280; Fax: 34-934-021-219; E-mail: fciruela@ub.edu.

[3] The abbreviations used are: NMDA, *N*-methyl-D-aspartic acid; mGlu, metabotropic glutamate; PSD, postsynaptic density; GST, glutathione S-transferase; FRET, fluorescence resonance energy transfer; YFP, yellow fluorescent protein; HRP, horseradish peroxidase; PBS, phosphate-buffered saline; CAMKII, Ca^{2+}/calmodulin-dependent protein kinase II; CaR, calcium-sensing receptor; MAPK, mitogen-activated protein kinase; ERK, extracellular signal-regulated kinase; MEK, MAPK/ERK kinase; MEKK, MEK kinase.

and 14). Members of the α-actinin family, namely α-actinin-1, -2, and -4, are abundantly represented in postsynaptic density (PSD) excitatory synapses (15, 16), where it is believed they regulate postsynaptic actin dynamics and spine morphology (17). Recently, the spatial expression of α-actinin-2 in the rat central nervous system has been analyzed. The highest levels of the protein are found in the striatum, cortex, and hippocampus, where α-actinin-2 interacts with both the NMDA subtype of glutamate receptor (18, 19) and the adenosine A_{2A} receptor (20). Also, α-actinin-1 showed a high expression level in neurons of striatum, whereas the cerebellum and other subcortical structures showed only weak labeling (21).

In the present study we carried out a GAL-4-based yeast two-hybrid screen to identify mGlu$_{5b}$ partners in adult brain. Using a C-terminal tail region of the receptor as bait we identified α-actinin-1 and -4 as novel binding partners of the mGlu$_{5b}$ receptor. We focus on the characterization of α-actinin-1-mGlu$_{5b}$ interaction, because both proteins are heavily expressed in the same adult brain area, the striatum. This interaction might have relevant physiological consequences, because we demonstrate, in the present work, that α-actinin-1 controls the cell surface expression and functioning of mGlu$_{5b}$ receptor.

EXPERIMENTAL PROCEDURES

Plasmid Constructs—Two EcoRI-XhoI fragments of the C-terminal tail of the mGlu$_{5b}$ receptor were subcloned into the bait vector pHybLexA/Zeo (Invitrogen). One fragment coding for amino acids 828–1006 (LmGlu$_{5b}$) was amplified using TaqDNA polymerase (Sigma) and the following primers: FLmGlu$_{5b}$ (5′-GGCTGGAATTCAAACCGGAGAGAAATGTGCG-3′) and RLmGlu$_{5b}$ (5′-GCCTCGAGTCACAGCGACGGCGCATC-3′). For the second fragment coding for amino acids 828–932 (SmGlu$_{5b}$) the following primers were used: RLmGlu$_{5b}$ (5′-AGACTCGAGGTCACAAATGTTGCCCCCGG-3′) and the same FLmGlu$_{5b}$.

Human α-actinin-1 cloned in the HindIII restriction site of pEYFP-N1 (Clontech) was kindly provided by Dr. Carol Otey, Dept. of Cell and Molecular Physiology, University of North Carolina, Chapel Hill. Several human α-actinin-1-GST fusion proteins were made by PCR amplification and cloning into the EcoRI/XhoI sites of pGEX-4T-1 (Amersham Biosciences) using the following primers: RFA1 (5′-CCGCTCGAGTTAGAGGTCACTCTCGCCGTACAGC-3′) and FFA1 (5′-CCGGAATTCATGGACCATTATGATTCTCAG-3′) for the fusion protein GST-α-actinin-1, RFA1 and FF1A1 (5′-CCGGAATTCACGGAGGAGCATGCCCGACAGCAGC-3′) for the fusion protein GST-α-actinin-1-(619–892), RFA1 and FF2A1 (5′-CCGGAATTCAATGAGTTCCGGGCCTCCTTCAACC-3′) for the fusion protein GST-α-actinin-1-(746–892), RFA1 and FF3A1 (5′-CCGGAATTCCGAGACAGCCGACACAGATACAGC-3′) for the fusion protein GST-α-actinin-1-(816–892), and FFA1 and RF4A1 (5′-CCGCTCGAGTCACGGGACATGAAGTCAATGAAGGCC-3′) for the fusion protein GST-α-actinin-1-(1–816). To perform FRET experiments the mGlu$_{5b}$ receptor was subcloned into the EcoRI/BamHI sites of pGFP^2-N3 vector (PerkinElmer Life Sciences) using the primers Fm5 (5′-CCCGTTGAATTCCTTTCCTAAAATG-3′) and Rm5 (5′-CCGCCAGGATCCCGCAACGATGAAGAACT-3′) to generate the construct mGlu$_{5b}$-GFP^2. Also, four human α-actinin-1-YFP fusion proteins were made by PCR amplification and cloning into the HindIII sites of pEYFP-N1 (Clontech) using the following primers: Rmut (5′-CTGCAGAATTCGAAGCTTGAGGTC-3′) and Fmut1 (5′-CCCAAGCTTATGGAGATCCGGAGGCTGGAGCG-3′) for the fusion protein α-actinin-1-(358–892)-YFP, Rmut and Fmut2 (5′-CCCAAGCTTATGAACGAGTTCCGGGCCTCCTTCAA-3′) for the fusion protein α-actinin-1-(746–892)-YFP and Rmut and Fmut3 (5′-CCCAAGCTTATGTCCCGCGAGACAGCCGACACAG-3′) for the fusion protein α-actinin-1-(816–892)-YFP, Fmut4 (5′-CCCAAGCTTATGGACCATTATGATTCTCAGC-3′) and Rmut4 (5′-CCCAAGCTTGTCAATGAAGGCCTGGAATGTC-3′) for the fusion protein α-actinin-1-(1–815)-YFP.

Yeast Two-hybrid System—Yeast two-hybrid screening was performed as described previously (20). Briefly, a bait strain was created by transforming pHybLex-LmGlu$_{5b}$ into *Saccharomyces cerevisiae* strain L40 as described in the manufacturer's instructions (Hybrid Hunter, Invitrogen). The bait strain was co-transformed with an adult mouse brain cDNA library constructed in the Gal4-activating domain vector pPC86 (Invitrogen), and transformants were plated onto minimal yeast media lacking histidine, tryptophan, uracil, and lysine, containing 300 mg/ml Zeocin (Invitrogen) and 5 mM 3-aminotriazole. Plates were incubated at 30 °C for 5 days, and yeast colonies that grew on histidine-deficient media were re-streaked onto fresh selective plates and assayed for β-galactosidase activity as per the manufacturer's instructions. Prey plasmids were isolated from yeast and electroporated into *Escherichia coli* XL-1Blue electrocompetent cells (Stratagene). The 5′-end of each clone was sequenced using a vector primer. To confirm the interaction in yeast, purified prey plasmids were re-transformed with the pHybLex-LmGlu$_{5b}$ and pHybLex-SmGlu$_{5b}$ baits and with the bait empty bait vector pHybLex/Zeo and tested for growth on selective plates and β-galactosidase activity.

For liquid β-galactosidase assays 1.5 ml of each culture, grown for 48 h at 30 °C, was spun, and the pellet was re-suspended in 200 μl of Z buffer (60 mM Na_2HPO_4, 40 mM NaH_2PO_4, 10 mM KCl, 1 mM $MgSO_4$, pH 7.0). A small amount of glass beads (425–600 μm, Sigma) was added, and the mixture was sonicated for 5–10 min. After cell lysis, the samples were spun to pellet the cell debris. 100 μl of supernatant was transferred to a new microcentrifuge tube, and 700 μl of Z buffer containing β-mercaptoethanol (27 μl/10 ml) was added. 150 μl of 2.5 mg/ml *ortho*-nitrophenyl-β-galactoside (Sigma) was added to the sample, and the mixture was incubated at 37 °C for 3 h. The absorbance was read at 420 nm and referred to the amount of protein present in each sample. For strong enzymatic reactions (*i.e.* when the color started to appear after a few minutes of incubation), a 1:10 dilution of the yeast lysate was used and the absorbance at 420 nm was multiplied by 10.

Antibodies—The primary antibodies were: rabbit anti-mGlu$_{5a/b}$ receptor polyclonal antibody (Upstate), rabbit anti-α-actinin polyclonal antibody (Santa Cruz Biotechnology, Santa Cruz, CA), mouse anti-α-actinin monoclonal antibody (Sigma), mouse anti-NR1 monoclonal antibody (Upstate), rabbit anti-GST polyclonal antibody (22), mouse anti-GFP monoclonal

antibody (Sigma), rabbit anti-extracellular signal-regulated kinase (ERK) 1/2 polyclonal antibody (clone M-5670, Sigma), mouse anti-phosphorylated ERK1/2 (clone M-8159, Sigma), and mouse anti-calnexin monoclonal antibody (BD Transduction Laboratories). The secondary antibodies were: horseradish-peroxidase (HRP)-conjugated goat anti-rabbit IgG (Pierce), HRP-conjugated anti-rabbit IgG TrueBlot™ (eBioscience), HRP-conjugated rabbit anti-mouse IgG (Dako), Texas red-conjugated goat anti-rabbit IgG (Molecular Probes), and AlexaFluor488-conjugated goat anti-mouse IgG (Molecular Probes).

Cell Culture, Transfection, and Membrane Preparation—HEK-293 cells were grown in Dulbecco's modified Eagle's medium (Sigma) supplemented with 1 mM sodium pyruvate, 2 mM L-glutamine, 100 units/ml penicillin/streptomycin, and 10% (v/v) fetal bovine serum at 37 °C and in an atmosphere of 5% CO_2. HEK-293 cells growing in 25-cm^3 dishes or 20-mm coverslips were transiently transfected with 10 μg of DNA encoding for the proteins specified in each case by calcium phosphate precipitation (23). The cells were harvested at either 24 or 48 h after transfection.

Neuronal striatal primary cultures were obtained as described previously (24) and plated at a density of 5×10^4 cells/cm^2. Membrane suspensions from rat striatum or from transfected HEK cells were obtained as described previously (25, 26).

Gel Electrophoresis and Immunoblotting—SDS-PAGE was performed using 7.5 or 10% polyacrylamide gels. Proteins were transferred to polyvinylidene difluoride membranes using a semi-dry transfer system and immunoblotted with the indicated antibody and then HRP-conjugated goat anti-rabbit IgG (1/60,000), HRP-conjugated rabbit anti-goat IgG (1/60,000), or HRP-conjugated anti-rabbit IgG TrueBlot™ (1/1,000). The immunoreactive bands were developed using a chemiluminescent detection kit (Pierce) (27).

Expression of GST Fusion Proteins and Pull-down Assays—Recombinant fusion proteins GST, GST-α-actinin-1, GST-α-actinin-1-(1–816), GST-α-actinin-1-(619–892), GST-α-actinin-1-(746–892), and GST-α-actinin-1-(816–892) were expressed in the *E. coli* BL21 strain (Invitrogen) with 0.1 mM isopropyl-β-D-thiogalactopyranoside (Sigma) for 3 h at 37 °C and purified on glutathione-Sepharose (Amersham Biosciences) as described previously (22). 5 μg of each fusion protein was coupled to 100 μl of a 50% suspension (v/v) of glutathione-agarose beads (Sigma) in PBS for 1 h at 4 °C. Membranes from HEK-293 transiently transfected with the mGlu$_{5b}$ receptor were solubilized in ice-cold lysis buffer (PBS, pH 7.4, containing 1% (v/v) Nonidet P-40) for 30 min at 4 °C. The solubilized material was centrifuged at 14,000 × *g* for 20 min, and the supernatant was pre-cleared with 100 μl of the 50% suspension (v/v) of glutathione-agarose beads for 1 h with constant rotation at 4 °C. After the pre-clearing, supernatants were transferred to a clean tube containing GST, GST-α-actinin-1, GST-α-actinin-1-(1–816), GST-α-actinin-1-(619–892), GST-α-actinin-1-(746–892), or GST-α-actinin-1-(816–892) coupled to the glutathione-agarose and incubated overnight with constant rotation at 4 °C. Subsequently, the beads were washed twice with ice-cold lysis buffer, twice with ice-cold lysis buffer containing 0.1% (v/v) Nonidet P-40, and once with PBS and aspirated to dryness with a 28-gauge needle. Subsequently, 30 μl of SDS-PAGE sample buffer (8 M urea, 2% SDS, 100 mM dithiothreitol, 375 mM Tris, pH 6.8) was added to each sample. Immune complexes were dissociated by heating to 37 °C for 2 h and resolved by SDS-PAGE in 7.5% gels and immunoblotted as described above.

Immunoprecipitation and Immunocytochemistry—For immunoprecipitation, membranes from transiently transfected HEK cells were solubilized in ice-cold lysis buffer (PBS, pH 7.4, containing 1% (v/v) Nonidet P-40) for 30 min on ice. In the case of rat striatum membranes these were solubilized in 2% SDS in PBS and then diluted with 5 volumes of ice-cold 2% (v/v) Nonidet P-40 in PBS (28). In both cases, the solubilized preparation was then centrifuged at 13,000 × *g* for 30 min. The supernatant (1 mg/ml) was processed for immunoprecipitation, each step of which was conducted with constant rotation at 0–4 °C. The supernatant was incubated overnight with the indicated antibody. Next 40 μl of a suspension of protein G cross-linked to agarose beads was added, and the mixture was incubated overnight. The beads were washed and treated as described above.

For immunocytochemistry, transiently transfected HEK-293 cells, or rat neuronal striatal primary cultures, were fixed in 4% paraformaldehyde for 15 min, and washed with PBS containing 20 mM glycine (buffer A) to quench the remaining free aldehyde groups. Cells were permeabilized with buffer A containing 0.2% Triton X-100 for 5 min. Blocking was performed using buffer A containing 1% bovine serum albumin (buffer B). Cells were labeled for 1 h at room temperature with the indicated primary antibody, washed for 30 min in buffer B, and stained with the corresponding secondary antibodies for another hour. Samples were rinsed and then examined using a confocal microscope (29, 30). To test the specificity of the antibodies we omitted or replaced the primary antibodies with buffer B. Under these conditions, no selective labeling was observed.

FRET Experiments Analyzed by Fluorometry—Forty-eight hours after transfection, cells were rapidly washed twice in PBS, detached, and re-suspended in the same buffer. To control the number of cells, the protein concentration of the samples was determined using a Bradford assay kit (Bio-Rad) using bovine serum albumin dilutions as standards. Cell suspension (20 μg of protein) was distributed in duplicate into 96-well microplates (black plates with a transparent bottom). Plates were read in a Fluostar Optima Fluorometer equipped with a high energy xenon flash lamp, using a 10 nm bandwidth excitation filter at 400 nm (393–403 nm), and 10 nm bandwidth emission filters corresponding to a 506–515 nm filter (Ch 1) and a 527–536 nm filter (Ch 2). Gain settings were identical for all experiments to keep the relative contribution of the fluorophores to the detection channels constant for spectral un-mixing. Quantitation of FRET was performed as described previously (31). The contribution of each fluorophore to both detection channels was calculated from the readings obtained by expressing each GFP variant separately. The spectral signatures of the different receptors fused to either GFP[2] or YFP did not significantly vary from the determined spectral signatures of the fluorescent proteins alone. Linear un-mixing was performed according to Zim-

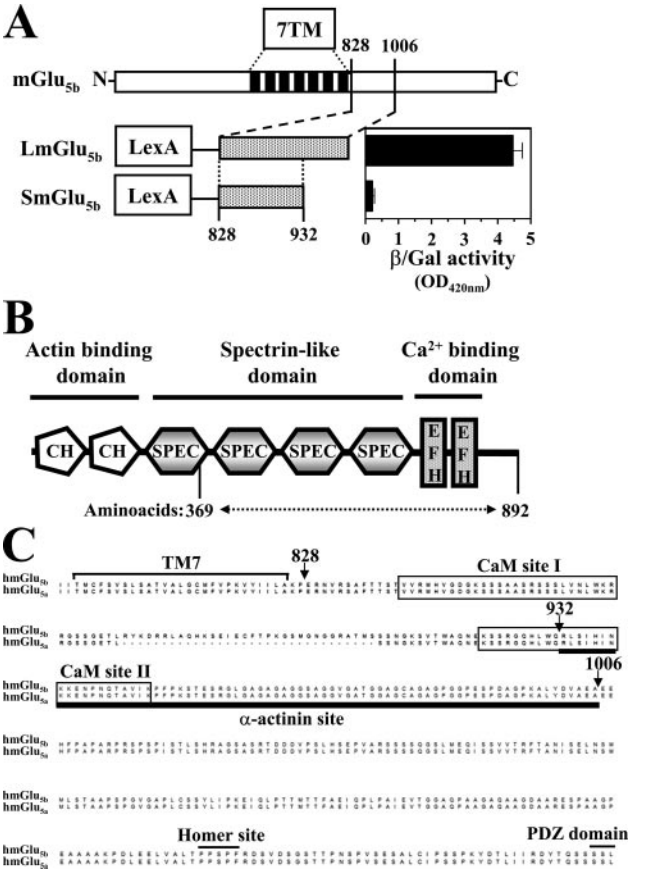

FIGURE 1. **α-Actinin-1 interacts with mGlu$_{5b}$ receptor in the yeast two-hybrid system.** *A*, schematic representation of the pHybLex-LmGlu$_{5b}$ (*LmGlu$_{5b}$*) fusion protein containing amino acids 828–1006 and pHybLex-SmGlu$_{5b}$ (*SmGlu$_{5b}$*) fusion protein containing amino acids 828–932 of the C-terminal tail mGlu$_{5b}$ receptor. Quantitation of the interaction of α-actinin-1 isoform with mGlu$_{5b}$ receptor fusion proteins was determined using a liquid β-galactosidase assay as described under "Experimental Procedures" (*inset panel* in *A*). Data are mean ± S.E. values of three replicates. *pHyb*, pHybLex (Invitrogen); *TM7*, seven transmembrane domains. *B*, schematic representation of the interacting region of α-actinin-1. The interacting region of α-actinin-1 with the C-Terminal tail mGlu$_{5b}$ receptor comprises amino acids 369–892 of α-actinin-1. *CH*, calponin homology domain; *SPEC*, spectrin-like motif; *EFH*, EF-hand domain. *C*, the regions containing transmembrane 7 (*TM7*) and C-terminal tail of hmGlu$_{5b}$ (accession code: D28539) and hmGlu$_{5a}$ (accession code: D28538) are aligned. *Dashed lines* indicate the region of deletions in the hmGlu$_{5a}$ (32 amino acids) receptor variant. The putative α-actinin-1 binding motif is *underlined* in *black* (amino acids 932–1006). The *two boxed regions* represent the Ca^{2+}/calmodulin binding motifs. Also illustrated are motifs required for Homer and PDZ domain interactions.

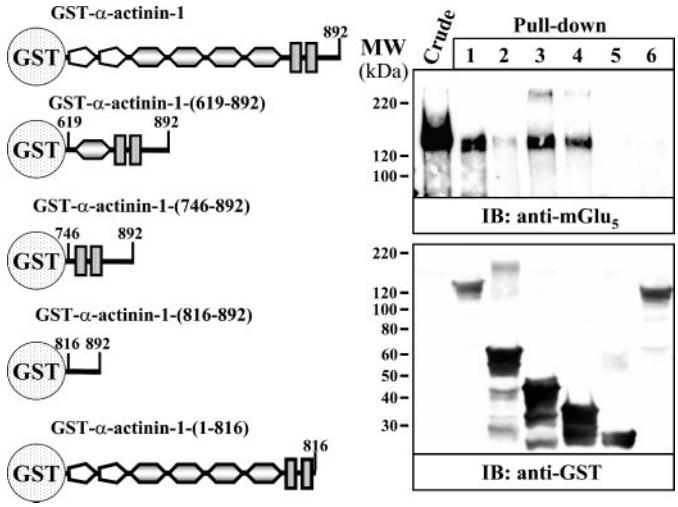

FIGURE 2. **Mapping of the mGlu$_{5b}$ receptor interaction site of α-actinin-1.** On the *left* are shown the α-actinin-1 GST fusion proteins used in the pull-down experiments. Transiently expressed mGlu$_{5b}$ receptor in HEK-293 cells extracts (*Crude*) was pulled down with GST-α-actinin-1 (*lane 1*), GST-α-actinin-1-(619–892) (*lane 2*), GST-α-actinin-1-(746–892) (*lane 3*), GST-α-actinin-1-(816–892) (*lane 4*), GST alone (*lane 5*), and GST-α-actinin-1-(1–816) (*lane 6*). mGlu$_{5b}$ receptor was detected using a polyclonal antibody against the mGlu$_{5a/b}$ receptor (1/1,000), and the GST fusion proteins with a polyclonal antibody were used against GST (1/2,000). The primary bound antibody was detected using a HRP-conjugated goat anti-rabbit antibody (1/60,000). The immunoreactive bands were visualized by chemiluminescence.

mermann *et al.* (32) and was used to determine the fluorescence emitted by each of the fluorophores.

Biotinylation of Cell Surface Proteins—Cell surface proteins were biotinylated as described previously (33, 34). Briefly, HEK-293 cells transiently transfected with the mGlu$_{5b}$ receptor in the absence, or presence, of α-actinin-1-YFP constructs were washed three times in borate buffer (10 mM H_3BO_3, pH 8.8; 150 mM NaCl) and then incubated with 50 μg/ml Sulfo-NHS-LC-Biotin (Pierce) in borate buffer for 5 min at room temperature. Cells were washed three times in borate buffer and again incubated with 50 μg/ml Sulfo-NHS-LC-Biotin in borate buffer for 10 min at room temperature, and then 13 mM NH_4Cl was added for 5 min to quench the remaining biotin. Cells were washed in Tris-buffered saline, disrupted with three 10-s strokes in a Polytron, and centrifuged at 14,000 × *g* for 30 min. The pellet was solubilized in ice-cold lysis buffer (see above) for 30 min and centrifuged at 14,000 × *g* for 20 min. The supernatant was incubated with 80 μl of streptavidin-agarose beads (Sigma) for 1 h with constant rotation at 4 °C. The beads were washed and treated as described above and processed for immunoblotting.

Extracellular Signal-regulated Kinase Assay—Before stimulation with quisqualic acid transiently transfected HEK-293 cells were serum-starved for 16 h by replacing the usual culture medium for normal Dulbecco's modified Eagle's medium without glutamine and fetal bovine serum but containing 2 mM sodium pyruvate and 1 unit/ml glutamate-pyruvate transaminase (Roche Applied Science) to eliminate glutamate from the medium. After stimulation, cells were washed with ice-cold PBS and scraped into 1 ml of lysis buffer containing 1% Triton X-100, 50 mM Tris-HCl, pH 7.6, 45 mM β-glycerophosphate, 50 mM NaF, and 1 mM $NaVO_4$ in the presence of a protease inhibitor mixture (Sigma). Lysed cells were centrifuged for 20 min at 14,000 rpm at 4 °C, and equal protein concentrations were resolved on 10% SDS-PAGE, blotted onto Immobilon-P membrane, and incubated with rabbit anti-ERK1/2 (1/40,000) or mouse anti-phospho-ERK1/2 (1/2,500). Quantitative analysis of detected bands was performed by using densitometric scanning (35).

RESULTS

Yeast Two-hybrid Screening—To identify intracellular proteins interacting with the mGlu$_{5b}$ receptor, a region containing 178 amino acids of the C-terminal tail of the receptor (amino acids 828–1006) were fused in-frame with LexA in the pHybLexA/Zeo vector (LmGlu$_{5b}$, Fig. 1*A*) and used to screen a mouse brain cDNA library using the yeast two-hybrid system. Of the seven clones, from the 1 × 10^6 total transfor-

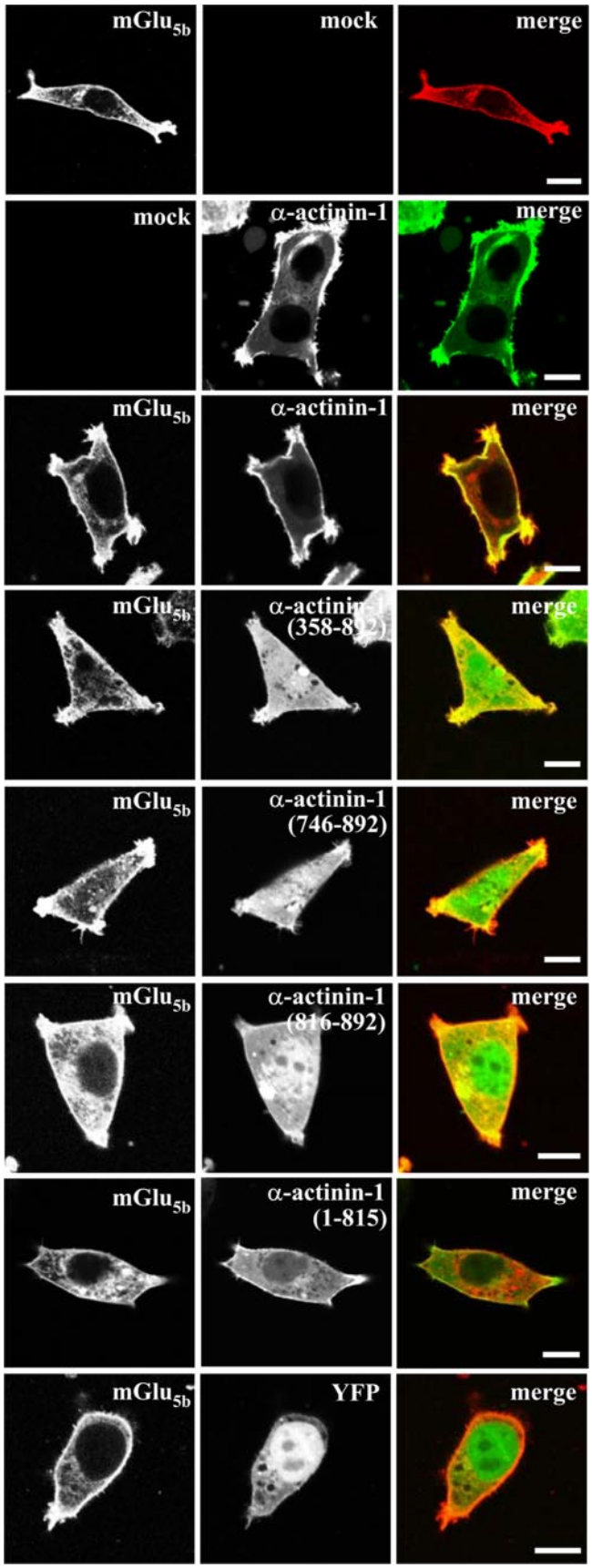

FIGURE 3. **Co-expression of mGlu$_{5b}$ receptor and α-actinin-1 constructs in HEK-293 cells.** HEK-293 cells were transiently transfected with mGlu$_{5b}$ receptor alone, α-actinin-1-YFP alone, mGlu$_{5b}$ receptor plus α-actinin-1-YFP, mGlu$_{5b}$ receptor plus α-actinin-1-(358–892)-YFP, mGlu$_{5b}$ receptor plus α-actinin-1-(746–892)-YFP, mGlu$_{5b}$ receptor plus α-actinin-1-(816–892)-YFP, mGlu$_{5b}$ receptor plus α-actinin-1-(1–815)-YFP or mGlu$_{5b}$ receptor plus YFP. Cells were processed for immunocytochemistry (see "Experimental Procedures") using a polyclonal antibody against mGlu$_{5a/b}$ receptor (1/200) followed by Texas Red-conjugated goat anti-rabbit (1/2000). Cells were analyzed by double immunofluorescence with a confocal microscope. Superimposition of images (*merge*) reveal co-distribution of mGlu$_{5b}$ receptor with α-actinin-1 constructs in *yellow*. *Scale bar*, 10 μm.

mants screened that were found to grow onto nutritional-deficient plates and activated the β-galactosidase assay, three were identified as different isoforms of the actin binding protein α-actinin, one clone for α-actinin-1, and another two for α-actinin-4. The isolated α-actinin-1 clone comprises amino acids 369–892 that include part of the spectrin-like motif and the Ca^{2+} binding domain (Fig. 1*B*). To determine the region of the C-terminal domain of the mGlu$_{5b}$ receptor that interacted with α-actinin-1, another LexA fusion protein missing the last 74 amino acids of the former LmGlu$_{5b}$ was constructed (SmGlu$_{5b}$, Fig. 1*A*) and tested for its ability to bind α-actinin-1. This shorter fusion protein could not interact with α-actinin-1 as tested using a liquid β-galactosidase assay (Fig. 1*A*, *inset panel*), thus mapping the interacting domain to within amino acids 932–1006 of mGlu$_{5b}$ receptor. This region is common in both mGlu$_{5a}$ and mGlu$_{5b}$ receptor isoforms and close to the described Ca^{2+}/calmodulin binding motifs (36) (Fig. 1*C*).

α-Actinin-1 Binds to the C-terminal Domain of mGlu$_{5b}$ Receptor—By means of pull-down experiments we tested the ability of naturally expressed full-length mGlu$_{5b}$ receptor to associate with GST fusion proteins containing different regions of α-actinin-1 (Fig. 2, *left part*). As shown in Fig. 2, an immunoreactive band of ~130 kDa corresponding to the mGlu$_{5b}$ receptor could be detected in the crude extracts from HEK-293 cells transiently expressing the receptor (Fig. 2, *Crude*). This band was observed in pull-down assays when cell lysates were incubated with GST-α-actinin-1, GST-α-actinin-1-(619–892), GST-α-actinin-1-(746–892), and GST-α-actinin-1-(816–892) (Fig. 2, *lanes 1–4*, respectively), but was not detected either with GST-α-actinin-1-(1–816) fusion protein or with GST alone (Fig. 2, *lanes 6* and *5*, respectively). This result shows that the naturally expressed mGlu$_{5b}$ receptor binds specifically to a region in the α-actinin-1 protein located within amino acids 816 and 892. On the other hand, the binding of the mGlu$_{5b}$ receptor to this region was not altered by the presence of 2 mM Ca^{2+} or 5 mM EDTA (data not shown). Interestingly, this C-terminal region of α-actinin-1 (76 amino acids) displays 70% amino acid sequence identity (84% similarity) across the α-actinin-1, -2, and -3 isoforms (37) and contains a PDZ domain-binding sequence, ESDL (11).

Interaction of the mGlu$_{5b}$ Receptor and α-Actinin-1 in Transfected HEK-293 Cells and in Rat Striatum—The association of the mGlu$_{5b}$ receptor and α-actinin-1 was subsequently studied in transfected HEK-293 cells by double immunolabeling experiments and co-immunoprecipitation. By confocal microscopy analysis of HEK-293 cells transiently co-transfected with the cDNA encoding for the mGlu$_{5b}$ receptor and α-actinin-1-YFP, a marked overlap in the distribution of the two proteins was found at the plasma membrane level (Fig. 3). Interestingly,

when the double immunolabeling experiment was performed in HEK-293 cells transiently transfected with the cDNA encoding the mGlu$_{5b}$ receptor and either α-actinin-1-(358–892)-YFP, a-actinin-1-(746–892)-YFP, or α-actinin-1-(816–892)-YFP some co-distribution was observed at the plasma membrane, although most of the α-actinin-1 constructs showed a cytosolic and nuclear distribution. This latter distribution might arise, because all of the α-actinin-1 constructs are missing the calponin homology domain, which accounts for the binding to actin filaments. On the other hand, a mutant of the α-actinin-1 lacking the last 76 amino acids, namely α-actinin-1-(1–815)-YFP, showed a low level of co-distribution with mGlu$_{5b}$ besides this mutant was also expressed at the plasma membrane (Fig. 3). These results suggest that the putative mGlu$_{5b}$-interacting domain of α-actinin-1 is necessary to bring together these two proteins. Finally, when the mGlu$_{5b}$ receptor was co-transfected with YFP the co-distribution between these two proteins was very low (Fig. 3), suggesting that the co-distribution between the mGlu$_{5b}$ receptor, α-actinin-1-YFP, and its deleted constructs is indeed specific. When cell extracts of HEK-293 cells transiently transfected with the mGlu$_{5b}$ receptor plus α-actinin-1-YFP, α-actinin-1-(358–892)-YFP, α-actinin-1-(746–892)-YFP, or α-actinin-1-(816–892)-YFP were immunoprecipitated with an antibody against GFP and these immunoprecipitates were analyzed by Western blot using an antibody against the mGlu$_{5a/b}$ receptor, a band of 130 kDa, which corresponds to the mGlu$_{5b}$ receptor, was observed (Fig. 4, *bottom panel*, *lanes 1–4*). Interestingly, this band did not appear in immunoprecipitates from cells co-transfected with mGlu$_{5b}$ receptor plus YFP (Fig. 4, *bottom panel*, *lane 5*) or from cells co-transfected with mGlu$_{5b}$ receptor plus α-actinin-1-(1–815)-YFP (Fig. 4, *bottom panel*, *lane 6*), suggesting again that the region comprised between amino acids 816 and 892 of α-actinin-1 is responsible for the interaction with mGlu$_{5b}$ receptor.

The protein-protein interaction between the mGlu$_{5b}$ receptor and α-actinin-1 was determined by a FRET approach using the mGlu$_{5b}$-GFP^2 and α-actinin-1-YFP pair (see "Experimental Procedures"). FRET efficiency was determined to be ~27% (Fig. 5). The relatively low FRET efficiency (~33%) of a negative control constituted by the pair mGlu$_{5b}$-GFP^2 and YFP is consistent with a specific energy transfer between mGlu$_{5b}$-GFP^2 and α-actinin-1-YFP (FRET efficiency ~61%) (Fig. 5). Furthermore the FRET efficiency between mGlu$_{5b}$-GFP^2 and either α-actinin-1-(358–892)-YFP, α-actinin-1-(746–892)-YFP, or α-actinin-1-(816–892)-YFP was significantly higher than the negative control (Fig. 5). This is consistent with the stretch of α-actinin-1 amino acid sequence (amino acids 816–892) forming a direct interaction with the mGlu$_{5b}$ receptor. Interestingly, with the smaller α-actinin-1 construct, α-actinin-1-(816–892)-YFP, a marked increase in FRET efficiency was observed when compared with the other constructs, probably due it to its higher expression, easier access, and therefore closer contact to the receptor. Under the same experimental conditions, the α-actinin-1-(1–815)-YFP, the α-actinin-1 mutant lacking the last 76 amino-acids, showed a FRET efficiency similar to that observed for the pair mGlu$_{5b}$-GFP^2 and YFP (negative control) (Fig. 5). Together, these results demonstrate that α-actinin-1 can interact with mGlu$_{5b}$ receptor in a heterologous system and that the interaction is mediated by the last 76 amino acids (amino acids 816–892).

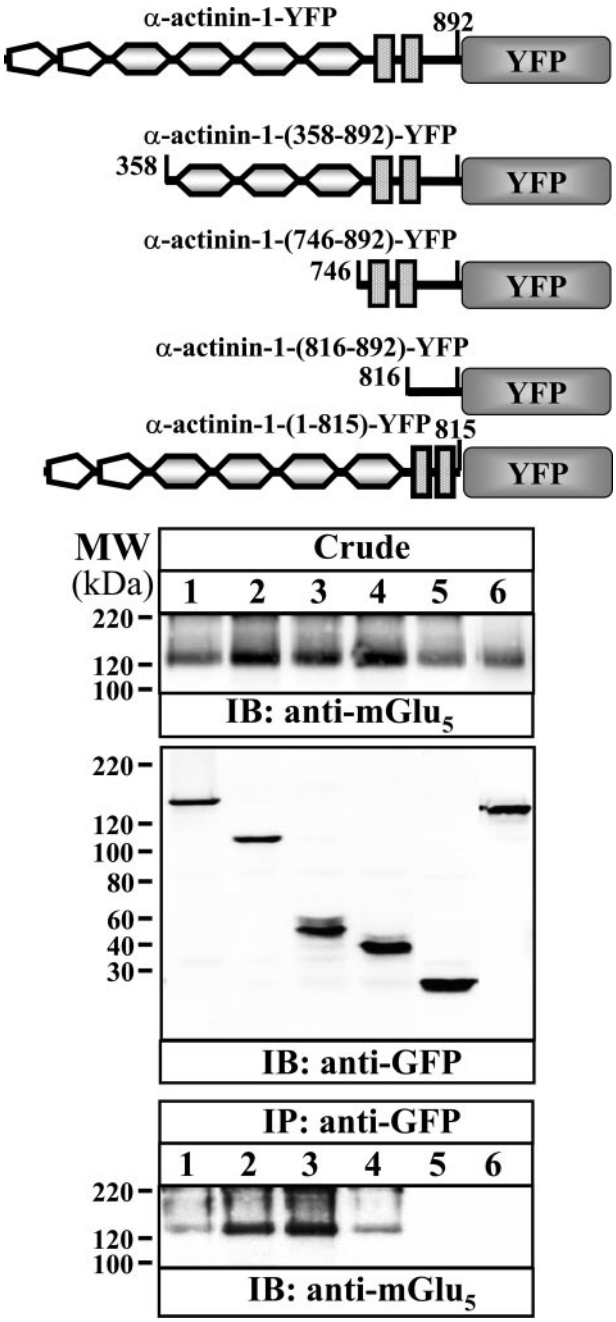

FIGURE 4. **Co-immunoprecipitation of mGlu$_{5b}$ receptor and α-actinin-1 constructs in HEK-293 cells.** HEK-293 cells were transiently transfected with mGlu$_{5b}$ receptor and α-actinin-1-YFP (*lane 1*), α-actinin-1-(358–892)-YFP (*lane 2*), α-actinin-1-(746–892)-YFP (*lane 3*), α-actinin-1-(816–892)-YFP (*lane 4*), YFP alone (*lane 5*), and α-actinin-1-(1–815)-YFP (*lane 6*). Cells were processed for immunoprecipitation (see "Experimental Procedures") using a monoclonal anti-GFP antibody (2 μg/ml). The crude extracts (*Crude*) and immunoprecipitates (*IP*: anti-GFP) were analyzed by SDS-PAGE and immunoblotted using a polyclonal antibody against mGlu$_{5a/b}$ receptor (1/1,000) and a monoclonal anti-GFP antibody (1/2,000). The primary bound antibody was detected using a HRP-conjugated goat anti-rabbit antibody (1/60,000) or HRP-conjugated rabbit anti-mouse antibody (1/6,000). The immunoreactive bands were visualized by chemiluminescence.

To assess the physiological relevance of the α-actinin-1/mGlu$_{5b}$ receptor interaction, co-immunoprecipitation experi-

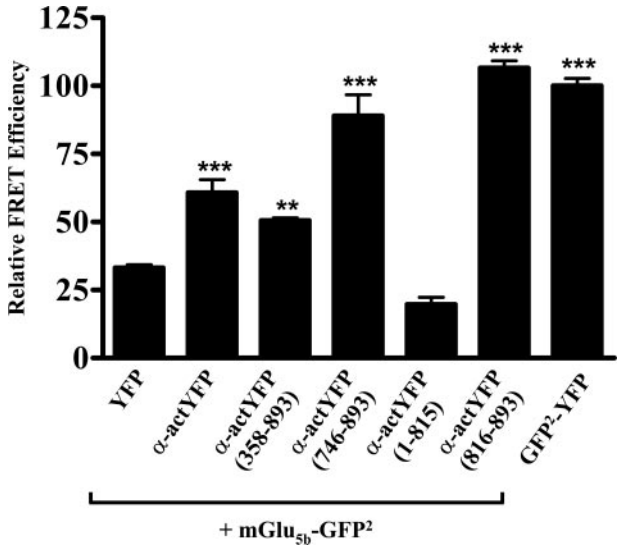

FIGURE 5. **FRET efficiency of the mGlu$_{5b}$-GFP^2 and α-actinin-YFP pair by sensitized emission in living cells.** HEK-293 cells were transiently transfected with the plasmids encoding the mGlu$_{5b}$-GFP^2 (donor) and the α-actinin-1-YFP constructs (acceptor) using a ratio of donor to acceptor DNA of 1:2. The α-actinin-1-YFP constructs used in the co-transfection were the same used in Fig. 3. The plasmid encoding the construct GFP^2-YFP was transfected and used as a positive control. Fluorescence readings were performed 48 h post transfection as described under "Experimental Procedures." Linear unmixing of the emission signals was applied to the data (see "Experimental Procedures"), and the results are shown as the sensitized emission of the acceptor when the cells were excited at 400 nm. Data are the mean ± S.D. of five to nine independent experiments performed in triplicate. Data of the different transfection groups were analyzed by one-way analysis of variance followed by Newman-Keuls post-hoc comparisons. **, $p < 0.05$ or ***, $p < 0.001$ *versus* the mGlu$_{5b}$-GFP^2 and YFP co-transfected cells (negative control).

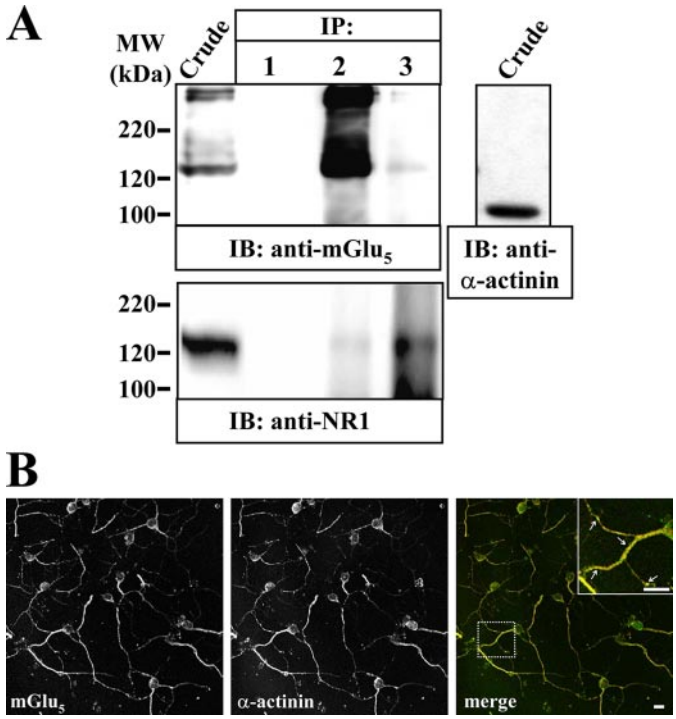

FIGURE 6. ***In vivo* interaction of mGlu$_5$ receptor and α-actinin in rat striatum.** *A*, solubilized extracts from rat striatum (see "Experimental Procedures") were subjected to immunoprecipitation analysis using nonspecific rabbit IgG (*lane 1*), rabbit anti-mGlu$_{5a/b}$ receptor antibody (2 μg/ml) (*lane 2*), and rabbit anti-α-actinin (2 μg/ml) (*lane 3*). Extracts (*Crude*) and/or immunoprecipitates (*IP*) were analyzed by SDS-PAGE and immunoblotted using a polyclonal antibody against mGlu$_{5a/b}$ receptor (1/1000), a monoclonal antibody against NR1 (1/1000), and a polyclonal antibody against α-actinin (1/1000). The primary bound antibody against NR1 was detected using a HRP-conjugated rabbit anti-mouse antibody (1/6000) and the anti-mGlu$_{5a/b}$ receptor antibody was detected using a HRP-conjugated anti-rabbit IgG TrueBlot™ (1/2000) to avoid IgG cross-reactivity. The immunoreactive bands were visualized by chemiluminescence. *B*, primary cultures of rat striatum neurons (DIV 14–21) were cultured and processed for immunocytochemistry (see "Experimental Procedures") using a polyclonal antibody against mGlu$_{5a/b}$ receptor (1/200) and a monoclonal anti-α-actinin antibody (1/100) followed by Texas red-conjugated goat anti-rabbit (1/2000) and AlexaFluor488-conjugated goat anti-mouse IgG (1/1000). Cells were analyzed by double immunofluorescence with a confocal microscope. Superimposition of images (*merge*) reveals co-distribution in *yellow* (*arrow* in the *inset panel*). *Scale bar*: 10 μm.

ments on adult rat striatal homogenates and double immunolabeling on primary cultures of rat striatum neurons were performed. Using soluble extracts from adult rat striatum, which had been shown by Western blotting to contain both α-actinin and the mGlu$_{5a/b}$ receptor (Fig. 6*A*), the anti-α-actinin antibody could co-immunoprecipitate a band ~130 kDa, which was detected using an anti-mGlu$_{5a/b}$ receptor antibody (Fig. 6*A*, *upper panel*, *lane 3*). This band did not appear when an irrelevant rabbit IgG was used for immunoprecipitation (Fig. 6*A*, *upper panel*, *lane 1*), showing that the reaction was specific and that the detected band might correspond mainly to mGlu$_{5b}$ receptor variant, because this is the major adult form expressed in striatum (5). Interestingly, when the same blot was reacted with an antibody against NR1 subunit of the NMDA-type glutamate receptor, a band of 130 kDa corresponding to this NMDA subunit was detected in the immunoprecipitate with the anti-α-actinin antibody (Fig. 6*A*, *lower panel*, *lane 3*), as expected (18, 19). Also, a similar faint band was observed in the immunoprecipitate with the anti-mGlu$_{5a/b}$ antibody (Fig. 6*A*, *lower panel*, *lane 2*), suggesting that NMDA receptor might be somehow physically associated to the mGlu$_{5a/b}$ receptor in rat striatum.

The distribution of α-actinin and the mGlu$_{5a/b}$ receptor in primary rat striatal neurons was also analyzed using confocal microscopy analysis, and a similar punctate distribution and some degree of co-distribution for both proteins were found (Fig. 6*B*). Co-distribution occurred mainly at specific aggregates in dendrites (Fig. 6*B*, *arrows* in *inset panel*). Interestingly, the single labels for mGlu$_{5a/b}$ or for α-actinin give the same pattern as seen in the double co-staining (*i.e.* simultaneous detection of mGlu$_5$ plus α-actinin), suggesting that the co-immunodetection is indeed specific (data not shown). These observations are consistent with the concept that α-actinin and mGlu$_{5a/b}$ receptor associate in striatal neurons.

α-Actinin-1 Promotes Cell Surface Expression of mGlu$_{5b}$ Receptor—To gain insight into the physiological consequences of the α-actinin-1/mGlu$_{5b}$ receptor interaction, the effect of α-actinin-1 on the mGlu$_{5b}$ receptor cell surface expression was studied. To this end we isolated mGlu$_{5b}$ receptors present in the plasma membrane by cell surface protein biotinylation, using a membrane impermeant biotin ester, followed by streptavidin-agarose affinity precipitation of the membrane proteins. The results showed that the amount of mGlu$_{5b}$ receptor present at the cell surface is increased when mGlu$_{5b}$ receptor and α-actinin-1 are co-expressed, compared with the properties present when mGlu$_{5b}$ receptor is expressed alone (Fig. 7*A*, *Cell Surface*, *upper panel*, *lanes 6 versus 5*). Quantitation of

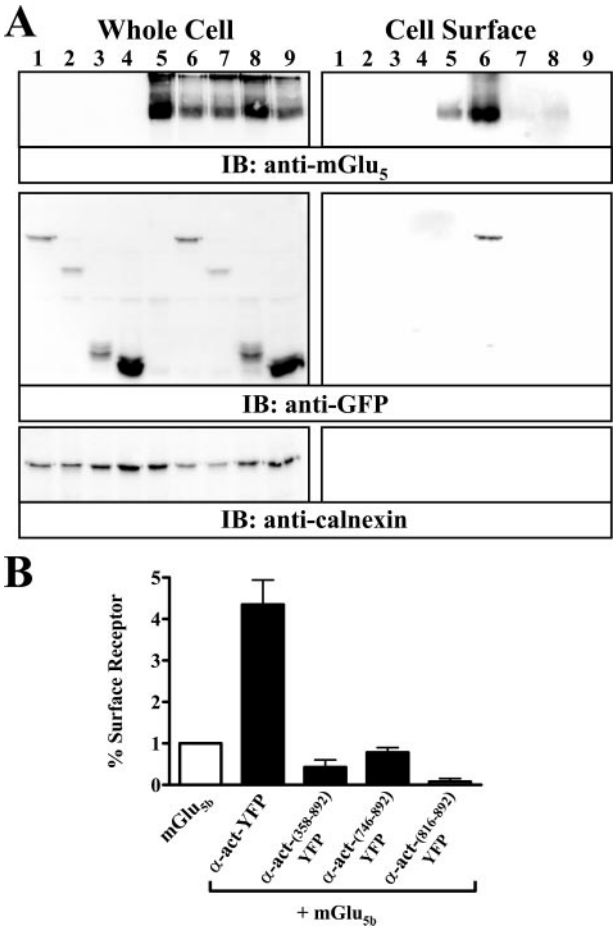

FIGURE 7. **Cell surface expression of mGlu$_5$ receptor in HEK-293 cells.** *A*, HEK-293 cells were transiently transfected with α-actinin-1-YFP (*lane 1*), α-actinin-(358–892)-YFP (*lane 2*), α-actinin-(746–892)-YFP (*lane 3*), α-actinin-(816–892)-YFP (*lane 4*), mGlu$_{5b}$ receptor alone (*lane 5*), mGlu$_{5b}$ receptor plus α-actinin-1-YFP (*lane 6*), mGlu$_{5b}$ receptor plus α-actinin-(358–892)-YFP (*lane 7*), mGlu$_{5b}$ receptor plus α-actinin-(746–892)-YFP (*lane 8*), or mGlu$_{5b}$ receptor plus α-actinin-(816–892)-YFP (*lane 9*). Cell surface labeling was performed as described under "Experimental Procedures." Crude extracts and biotinylated proteins were subsequently analyzed by SDS-PAGE and immunoblotted using a rabbit anti-mGlu$_5$ receptor antibody (1/1,000), a rabbit anti-α-actinin antibody (1/2,000), and a mouse anti-calnexin antibody (1/250). The primary bound antibody was detected using a HRP-conjugated goat anti-rabbit antibody (1/60,000) or HRP-conjugated rabbit anti-mouse antibody (1/6,000). The immunoreactive bands were visualized by chemiluminescence. *B*, quantification of cell surface receptor. The intensities of the immunoreactive bands on x-ray film corresponding to crude extracts and biotinylated protein were measured by densitometric scanning. Cell surface receptor values were normalized using the total amount of receptor in the crude extract for each sample. The results are presented as means ± S.E. of three independent experiments.

the increase of membrane bound/localized mGlu$_{5b}$ receptor indicated that the levels of surface receptor had risen by up to 4-fold in the α-actinin-1 co-transfected cells (Fig. 7*B*). Under similar conditions, when the mGlu$_{5b}$ receptor was co-transfected with α-actinin-1 mutants lacking the actin binding domain, *i.e.* α-actinin-1-(358–892)-YFP, α-actinin-1-(746–892)-YFP, and α-actinin-1-(816–892)-YFP, there was a reduction in plasma membrane mGlu$_{5b}$ receptor expression when compared with cells transfected with the mGlu$_{5b}$ receptor alone (Fig. 7*A*, *Cell Surface*, *upper panel*, *lanes 7–9 versus lane 5*). Interestingly, when the streptavidin isolates were reacted with the anti-GFP antibody to detect α-actinin-1 constructs, it became apparent that α-actinin-1 could be observed in the streptavidin isolates from the cells that were co-transfected with the mGlu$_{5b}$ receptor (Fig. 7, *Cell Surface*, *middle panel*, *lane 6*), suggesting that α-actinin-1 might be associated with the cell surface mGlu$_{5b}$ receptor. These results are in agreement with the marked overlap observed in the distribution of these two proteins found at the plasma membrane level (Fig. 3). Because no calnexin could be detected in the streptavidin isolates, it was clear that the biotin ester had not penetrated the cell membrane (Fig. 7, *Cell Surface*, *lower panel*). Because α-actinin-1 mutants lacking the domain responsible for the interaction with actin (calponin homology domain) inhibit receptor cell surface expression, these results suggest that the α-actinin-1-mediated-mGlu$_{5b}$ receptor plasma membrane expression requires the actin cytoskeleton.

Functional Implications of the mGlu$_{5b}$ Receptor-α-Actinin-1 Interaction—Recently, we have described that mGlu$_{5b}$ receptor can signal through the extracellular signal-regulated MAPK cascade (35). On the other hand, it has been shown that α-actinin isoforms interact with the MEK activator MEKK1 (38) or the extracellular signal-regulated kinase, ERK (39). To test the functional consequences of α-actinin-1/mGlu$_{5b}$ receptor interaction we studied the activation of the MAPK pathway by the mGlu$_{5b}$ receptor in HEK cells transiently expressing the mGlu$_{5b}$ receptor in the absence, or presence, of α-actinin-1 (receptor densities were controlled by immunoblotting, data not shown). Treatment with quisqualic acid (100 μM) did not induce ERK1/2 phosphorylation in cells transfected with α-actinin-1 alone. However, in cells transfected with the mGlu$_{5b}$ receptor alone quisqualic acid did induce a significant ERK1/2 phosphorylation, as expected (35). Interestingly, when cells were transiently transfected with both α-actinin-1 and the mGlu$_{5b}$ receptor a synergistic potentiation of ERK1/2 phosphorylation after receptor activation was observed (Fig. 8).

DISCUSSION

In this study, we have identified an interaction between the mGlu$_{5b}$ receptor and α-actinin-1 and have shown that this interaction can regulate cell surface expression and function of the receptor. A yeast two-hybrid screen was initially used to identify a novel interaction between the heptaspanning membrane mGlu$_{5b}$ receptor and the actin cross-linking protein α-actinin-1. This interaction was subsequently confirmed by means of pull-down experiments using GST and α-actinin-1-GST fusion constructs, and by co-distribution and co-immunoprecipitation experiments in transfected HEK-293 cells. Moreover, co-distribution of both proteins in rat striatum primary cultures and the ability of anti-α-actinin antibodies to immunoprecipitate mGlu$_5$ receptor from rat striatum homogenates suggest that the interaction is physiologically relevant.

α-Actinin-1 is a rod-shaped molecule composed of two 100-kDa anti-parallel monomers, linking actin filaments in a parallel way (Fig. 9). In the present work the mGlu$_{5b}$ receptor interacting region of α-actinin-1 was mapped within the last 76 amino acids of the molecule. Interestingly, for α-actinin-2, one of the two skeletal muscle isoforms of α-actinin that is also expressed in brain (18, 19), this domain is involved in the interaction with the Z repeats of titin in skeletal muscle (40, 41). Furthermore, the same 76 residues of α-actinin-2 have been

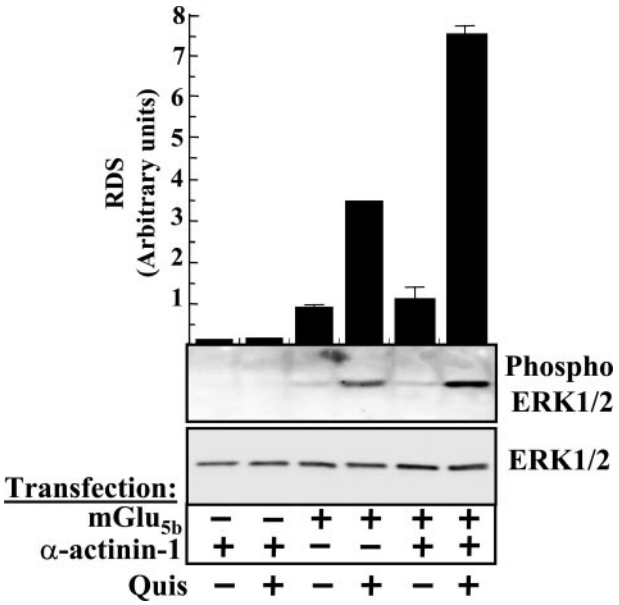

FIGURE 8. **Stimulation of ERK1/2 activity by mGlu$_{5b}$ receptor.** Serum-starved HEK cells expressing mGlu$_{5b}$ receptor in the absence or presence of α-actinin were stimulated with quisqualic acid (100 μM) for 5 min. The phosphorylation of ERK1/2 was determined by immunoblotting (see "Experimental Procedures"). *Bottom*, representative ERK assay; *top*, the intensities of the immunoreactive bands on x-ray film corresponding to ERK1/2 and phospho ERK1/2 protein were measured by densitometric scanning. All values of phosphorylated ERK1/2 were normalized using ERK1/2 and expressed as means ± S.E. (in relative densitometric scanning (*RDS*) obtained in non-treated transfected cells) of three independent experiments.

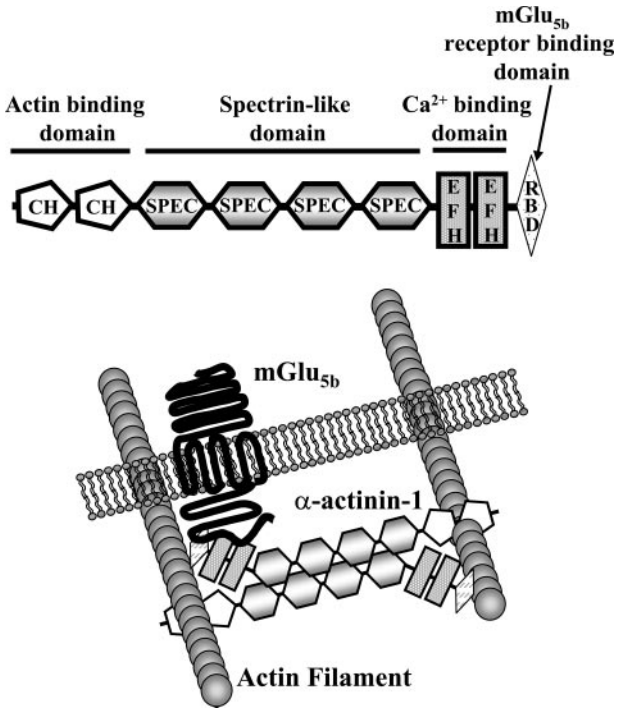

FIGURE 9. **Proposed model of α-actinin/mGlu$_5$ receptor interaction.** The *upper panel* shows a linear structure of α-actinin containing the calponin homology domains (*CH*), four spectrin-like motifs (*SPEC*), the EF-hand domains (*EFH*), and the receptor binding domain (*RBD*). The *lower panel* shows the proposed α-actinin/mGlu$_5$ receptor interacting model where α-actinin dimers link actin filaments in a parallel way and anchor the receptor to the plasma membrane.

shown to interact with ZASP (Z band alternately spliced PDZ-containing protein), another sarcomere Z disk protein (8, 42, 43). In the central nervous system, this region in the α-actinin-4 interacts with the PDZ (PSD-95, Dgl, Z0–1) domain of densin-180 and with Ca^{2+}/calmodulin-dependent protein kinase II (CaMKII), forming a ternary complex stabilized by multiple interactions (12, 37, 44). Also, for α-actinin-4 the same region is involved in the interaction with densin-180, a transmembrane protein that is tightly associated with the postsynaptic density in central nervous system neurons and that is postulated to function as a synaptic adhesion molecule (12). The PDZ domain of densin-180 contributes to its binding to α-actinin-4 (12). Furthermore, the C-terminal region of α-actinin-2 (amino acids 819–894), and the highly related proteins α-actinin-1 and α-actinin-4 interact with CaMKII (37). Apart from these interactions, the α-actinin family members also interact with cell surface receptors such as the Kv1-type potassium channel (45), the ATP-gated ion channel $P2X_7$ (46), and the glutamate NMDA receptor (47). α-Actinin binds to the NMDA receptor NR1 and NR2B subunit C termini at the C0 region, where it competes with calmodulin, which also binds NMDA receptors at the same site (48, 49). Displacement of α-actinin from the C0 region by calmodulin has been implicated in calcium-dependent inactivation of NMDA receptor-mediated whole cell currents (50). It has also been postulated that under resting cellular conditions α-actinin is bound to the NMDA receptor. This interaction predominantly decreases single channel closed time, resulting in an increased open probability (P_{open}). When the intracellular calcium concentration increases during neuronal excitation, calmodulin binds to, and α-actinin dissociates from, the receptor, causing an increase in mean channel closed time, a decrease in mean channel open time, and an overall reduction in P_{open} (51). It has also been suggested that the association of α-actinin with NMDA receptors may contribute to the NR2 subunit-selective modulation of this receptor, by localizing inactive CAMKII to the NMDA receptor (44, 52). In this context, it is interesting to note that an NMDA/α-actinin interaction has been reported in rat striatum (18, 19) where the mGlu$_{5a/b}$ receptor is also expressed. Furthermore, activation of mGlu$_{5a/b}$ receptors results in a pronounced potentiation of NMDA responses in several brain regions (53, 54), including the striatum (55), suggesting that mGlu/NMDA receptor interactions are of widespread significance. Indeed, cross-talk between type I mGlu and NMDA receptors has also been demonstrated in different types of central nervous system neurons, including cultured cortical neurons (56), cultured striatal neurons (57), and hippocampal CA3 pyramidal cells (58). The one or more mechanisms by which activation of mGlu$_{5a/b}$ receptor modulates NMDA receptor function are not well understood, and different hypotheses to explain the enhancement of NMDA currents by type I mGlu receptors have been proposed. For example, receptor-mediated phosphorylation of the NMDA receptor NR2A/B subunits by protein kinases, such as protein kinase C (56, 58), increases the open probability of the channel. Interestingly, NMDA receptor-mediated responses in layer V pyramidal neurons of the rat prefrontal cortex were facilitated by purinergic P2 receptor activation. The mechanisms underlying this facilitation implicated the activation of type I mGlu receptors,

namely mGlu$_1$ and mGlu$_{5a/b}$ receptors, via the G_q/phospholipase C/inositol 1,4,5-trisphosphate/Ca^{2+}/CAMKII transduction pathway (59).

It is important to note that the α-actinin domains mediating interactions with NMDA and mGlu$_{5a/b}$ receptors are different, meaning that simultaneous interaction of α-actinin with both receptors could take place. Under this scenario, the close association of NMDA and mGlu$_{5a/b}$ receptors would facilitate the modulation of NMDA receptor-mediated currents by the mGlu$_5$ receptor. On the other hand, it is also likely that the actin cytoskeleton, and α-actinin in particular, may have a role in the regulation of NMDA receptor function by the mGlu$_{5a/b}$ receptor in the rat striatum.

The presence of a complex involving the mGlu$_{5a/b}$ receptor and α-actinin suggests that α-actinin may mediate the association of the receptor with the actin cytoskeleton. Other studies have identified filamin A, another actin cross-linking protein similar to α-actinin, as an intracellular binding partner for other heptaspanning membrane receptors, namely the dopamine D_2 and D_3 receptors (60, 61), the calcium-sensing receptors (CaRs) (62), the metabotropic glutamate receptor 7 (63), the μ-opioid receptor (64), and the calcitonin receptor (65). Filamin A/D_2 receptor interaction is required for the proper targeting or stabilization of dopamine D_2 receptor at the plasma membrane (61, 66) and may contribute to its cell surface clustering (60). On the other hand, the interaction of CaR with filamin A prevents the degradation of the receptor, increasing its total cellular expression and plasma membrane localization, thus facilitating CaR signaling to the MAPK pathway (67). Furthermore, silencing the filamin A gene expression inhibits CaR signaling (68). In the case of the μ-opioid receptor its interaction with filamin A is required for proper trafficking and regulation of the receptor (64). The calcitonin receptor-filamin A interaction causes an increase in the recycling of the receptor to the cell surface and decreased degradation of the receptor, suggesting an important role for filamin in the endocytic sorting and recycling of the internalized calcitonin receptor (65). In contrast to the well documented interaction of filamin A with several heptaspanning membrane receptors, for α-actinin only one previous study has reported an interaction of this actin-binding protein with a G-protein-coupled receptor, namely the adenosine A_{2A} receptor (20). Here it was shown that the attachment of the A_{2A} receptor to the actin cytoskeleton through a direct interaction with α-actinin-2 is a pre-requisite for its agonist-induced plasma membrane clustering and β-arrestin-mediated internalization (20). Although the A_{2A} receptor was the first G-protein-coupled receptor documented to bind to an α-actinin isoform, namely the α-actinin-2, here we show that mGlu$_{5b}$ receptor also interacts with α-actinin-1 and that this interaction promotes cell surface expression of the receptor. Interestingly, this α-actinin-1-dependent cell surface expression of the receptor is maintained by the actin cytoskeleton, because mutants lacking the calponin homology domain, which renders them unable to bind actin, do not promote cell surface expression of the receptor.

α-Actinin isoforms also interact with proteins involved in signal transduction, such as the MEK activator MEKK1 or the extracellular signal-regulated kinase, ERK, as mentioned previously (38, 39). Also, mGlu$_{5b}$ receptor can signal through the extracellular signal-regulated MAPK cascade (35). Taking all this evidence together, it seems that α-actinin has a dual role as an actin cytoskeleton component and as a scaffolding protein, anchoring receptors to their target signaling molecules and thus ensuring a rapid and efficient signal transduction. A similar hypothesis has been suggested for filamin A, because this protein interacts with MEKs 1/2, p38 kinases (69), and the Ras-related GTPases, Rac, RhoA, Cdc42, and RalA (70). Also consistent with this double function as a scaffolding and an adaptor protein, the interaction of filamin A increases the coupling efficiency of the dopamine D_2 receptor with adenylate cyclase (60, 61) and is a prerequisite required for activation of MAPK signaling by the calcium-sensing receptor (67). Here we demonstrate, as for filamin A, that α-actinin-1 promotes mGlu$_5$ receptor signaling through the extracellular signal-regulated MAPK cascade, suggesting a functional role for the α-actinin-1/mGlu$_{5b}$ receptor interaction in addition to anchoring the receptor to the actin cytoskeleton.

In summary, a direct interaction between α-actinin-1 and mGlu$_{5b}$ receptor has been identified by using the yeast two-hybrid system and confirmed by convergent techniques in transfected HEK-293 cells and in more physiological models such as cultured neurons or rat striatum. Finally, we describe that the α-actinin-1-dependent cell surface expression of the receptor depends on the proper α-actinin-1 attachment to the actin cytoskeleton, facilitating the receptor coupling to the signal transduction machinery.

Acknowledgment—We are grateful to the personnel from Serveis Científic i Tècnics de la Universitat de Barcelona for their excellent technical assistance in confocal microscopy.

REFERENCES

1. Mayer, M. L., and Westbrook, G. L. (1987) *Prog. Neurobiol.* **28,** 197–276
2. Hollmann, M., and Heinemann, S. (1994) *Annu. Rev. Neurosci.* **17,** 31–108
3. Malenka, R. C., and Nicoll, R. A. (1993) *Trends Neurosci.* **16,** 521–527
4. Pin, J. P., and Duvoisin, R. (1995) *Neuropharmacology* **34,** 1–26
5. Romano, C., Smout, S., Miller, J. K., and O'Malley, K. L. (2002) *Neuroscience* **111,** 693–698
6. Bennett, V., and Gilligan, D. M. (1993) *Annu. Rev. Cell Biol.* **9,** 27–66
7. Lazarides, E., and Burridge, K. (1975) *Cell* **6,** 289–298
8. Faulkner, G., Pallavicini, A., Formentin, E., Comelli, A., Ievolella, C., Trevisan, S., Bortoletto, G., Scannapieco, P., Salamon, M., Mouly, V., Valle, G., and Lanfranchi, G. (1999) *J. Cell Biol.* **146,** 465–475
9. Castresana, J., and Saraste, M. (1995) *FEBS Lett.* **374,** 149–151
10. Davison, M. D., and Critchley, D. R. (1988) *Cell* **52,** 159–160
11. Trave, G., Pastore, A., Hyvonen, M., and Saraste, M. (1995) *Eur. J. Biochem.* **227,** 35–42
12. Walikonis, R. S., Oguni, A., Khorosheva, E. M., Jeng, C. J., Asuncion, F. J., and Kennedy, M. B. (2001) *J. Neurosci.* **21,** 423–433
13. Otey, C. A., and Carpen, O. (2004) *Cell Motil. Cytoskeleton* **58,** 104–111
14. Ciruela, F., Canela, L., Burgueno, J., Soriguera, A., Cabello, N., Canela, E. I., Casado, V., Cortes, A., Mallol, J., Woods, A. S., Ferre, S., Lluis, C., and Franco, R. (2005) *J. Mol. Neurosci.* **26,** 277–292
15. Walikonis, R. S., Jensen, O. N., Mann, M., Provance, D. W., Jr., Mercer, J. A., and Kennedy, M. B. (2000) *J. Neurosci.* **20,** 4069–4080
16. Peng, J., Kim, M. J., Cheng, D., Duong, D. M., Gygi, S. P., and Sheng, M. (2004) *J. Biol. Chem.* **279,** 21003–21011
17. Nakagawa, T., Engler, J. A., and Sheng, M. (2004) *Neuropharmacology* **47,** 734–745

18. Dunah, A. W., Wyszynski, M., Martin, D. M., Sheng, M., and Standaert, D. G. (2000) *Brain Res. Mol. Brain Res.* **79,** 77–87
19. Bouhamdan, M., Yan, H. D., Yan, X. H., Bannon, M. J., and Andrade, R. (2006) *J. Neurosci.* **26,** 2522–2530
20. Burgueño, J., Blake, D J., Benson, M. A., Tinsley, C. L., Esapa, C. T., Canela, E. I., Penela, P., Mallol, J., Mayor, F., Jr., Lluis, C., Franco, R., and Ciruela, F. (2003) *J. Biol. Chem.* **278,** 37545–37552
21. Kremerskothen, J., Teber, I., Wendholt, D., Liedtke, T., Bockers, T. M., and Barnekow, A. (2002) *Biochem. Biophys. Res. Commun.* **295,** 678–681
22. Ciruela, F., Burgueño, J., Casadó, V., Canals, M., Marcellino, D., Goldberg, S. R., Fuxe, K., Agnati, L. F., Lluis, C., Franco, R., Ferre, S., and Woods, A. (2004) *Anal. Chem.* **76,** 5354–5363
23. Jordan, M., Schallhorn, A., and Wurm, F. M. (1996) *Nucleic Acids Res.* **24,** 596–601
24. Chan, W. Y., Soloviev, M. M., Ciruela, F., and McIlhinney, R. A. (2001) *Mol. Cell. Neurosci.* **17,** 577–588
25. Casadó, V., Canti, C., Mallol, J., Canela, E. I., Lluis, C., and Franco, R. (1990) *J. Neurosci. Res.* **26,** 461–473
26. Burgueño, J., Enrich, C., Canela, E. I., Mallol, J., Lluis, C., Franco, R., and Ciruela, F. (2003) *J. Neurochem.* **86,** 785–791
27. Ciruela, F., and McIlhinney, R. A. J. (1997) *FEBS Lett.* **418,** 83–86
28. Müller, B. M., Kistner, U., Kindler, S., Chung, W. J., Kuhlendahl, S., Fenster, S. D., Lau, L. F., Veh, R.W., Huganir, R. L., Gundelfinger, E. D., and Garner, C. C. (1996) *Neuron* **17,** 255–265
29. Sarrió, S., Casadó, V., Escriche, M., Ciruela, F., Mallol, J., Canela, E. I., Lluis, C., and Franco, R. (2000) *Mol. Cell. Biol.* **20,** 5164–5174
30. Luján, R., and Ciruela, F. (2001) *Neuroreport* **12,** 1285–1291
31. Canals, M., Marcellino, D., Fanelli, F., Ciruela, F., De Benedetti, P., Goldberg, S. R., Fuxe, K., Agnati, L. F., Woods, A. S., Ferre, S., Lluis, C., Bouvier, M., and Franco, R. (2003) *J. Biol. Chem.* **278,** 46741–46749
32. Zimmermann, T., Rietdorf, J., Girod, A., Georget, V., and Pepperkok, R. (2002) *FEBS Lett.* **531,** 245–249
33. Ciruela, F., Soloviev, M. M., and McIlhinney, R. A. J. (1999) *Biochem. J.* **341,** 795–803
34. Burgueño, J., Canela, E. I., Mallol, J., Lluis, C., Franco, R., and Ciruela, F. (2004) *Exp. Cell Res.* **300,** 23–34
35. Ferré, S., Karcz-Kubicha, M., Hope, B. T., Popoli, P., Burgueño, J., Casadó, V., Fuxe, K., Lluis, C., Goldberg, S. R., Franco R., and Ciruela, F. (2002) *Proc. Natl. Acad. Sci. U. S. A.* **99,** 11940–11945
36. Minakami, R., Jinnai, N., and Sugiyama, H. (1997) *J. Biol. Chem.* **272,** 20291–20298
37. Robison, A. J., Bass, M. A., Jiao, Y., MacMillan, L .B., Carmody, L. C., Bartlett, R. K., and Colbran, R. J. (2005) *J. Biol. Chem.* **280,** 35329–35336
38. Christerson, L. B., Vanderbilt, C. A., and Cobb, M. H. (1999) *Cell Motil. Cytoskeleton* **43,** 186–198
39. Leinweber, B. D., Leavis, P. C., Grabarek, Z., Wang, C. L., and Morgan, K. G. (1999) *Biochem. J.* **344,** 117–123
40. Sorimachi, H., Freiburg, A., Kolmerer, B., Ishiura, S., Stier, G., Gregorio, C. C., Labeit, D., Linke, W. A., Suzuki, K., and Labeit, S. (1997) *J. Mol. Biol.* **270,** 688–695
41. Young, P., Ferguson, C., Banuelos, S., and Gautel, M. (1998) *EMBO J.* **17,** 1614–1624
42. Zhou, Q., Chu, P. H., Huang, C., Cheng, C. F., Martone, M. E., Knoll, G., Shelton, G. D., Evans, S., and Chen, J. (2001) *J. Cell Biol.* **155,** 605–612
43. Au, Y., Atkinson, R. A., Guerrini, R., Kelly, G., Joseph, C., Martin, S. R., Muskett, F. W., Pallavicini, A., Faulkner, G., and Pastore, A. (2004) *Structure* **12,** 611–622
44. Robison, A. J., Bartlett, R. K., Bass, M. A., and Colbran, R. J. (2005) *J. Biol. Chem.* **280,** 39316–39323
45. Cukovic, D., Lu, G. W., Wible, B., Steele, D. F., and Fedida, D. (2001) *FEBS Lett.* **498,** 87–92
46. Kim, M., Jiang, L. H., Wilson, H. L., North, R. A., and Surprenant, A. (2001) *EMBO J.* **20,** 6347–6358
47. Wyszynski, M., Lin, J., Rao, A., Nigh, E., Beggs, A. H., Craig, A. M., and Sheng, M. (1997) *Nature* **385,** 439–442
48. Ehlers, M. D., Zhang, S., Bernhardt, J. P., and Huganir, R. L. (1996) *Cell* **84,** 745–755
49. Zhang, S., Ehlers, M. D., Bernhardt, J. P., Su, C.-T., and Huganir, R. L. (1998) *Neuron* **21,** 443–453
50. Krupp, J. J., Vissel, B., Thomas, C. G., Heinemann, S. F., and Westbrook, G. L. (1999) *J. Neurosci.* **19,** 1165–1178
51. Rycroft, B. K., and Gibb, A. J. (2004) *J. Physiol.* **557,** 795–808
52. Sessoms-Sikes, S., Honse, Y., Lovinger, D. M., and Colbran, R. J. (2005) *Mol. Cell. Neurosci.* **29,** 139–147
53. Attucci, S., Carla, V., Mannaioni, G., and Moroni F. (2001) *Br. J. Pharmacol.* **132,** 799–806
54. Ugolini, A., Corsi, M., and Bordi, F. (1997) *Neuropharmacology* **36,** 1047–1055
55. Pisani, A., Calabresi, P., Centonze, D., and Bernardi, G. (1997) *Br. J. Pharmacol.* **120,** 1007–1014
56. Heidinger, V., Manzerra, P., Wang, X. Q., Strasser, U., Yu, S. P., Choi, D. W., and Behrens, M. M. (2002) *J. Neurosci.* **22,** 5452–5461
57. Yang, L., Mao, L., Tang, Q., Samdani, S., Liu, Z., and Wang, J. Q. (2004) *J. Neurosci.* **24,** 10846–10857
58. Benquet, P., Gee, C. E., and Gerber, U. (2002) *J. Neurosci.* **22,** 9679–9686
59. Wirkner, K., Gunther, A., Weber, M., Guzman, S. J., Krause, T., Fuchs, J., Koles, L., Norenberg, W., and Illes, P. (2006) *Cereb. Cortex* **17,** 621–631
60. Li, M., Bermak, J. C., Wang, Z. W., and Zhou, Q. Y. (2000) *Mol. Pharmacol.* **57,** 446–452
61. Lin, R., Karpa, K., Kabbani, N., Goldman-Rakic, P., and Levenson, R. (2001) *Proc. Natl. Acad. Sci. U. S. A.* **98,** 5258–5263
62. Hjälm, G., MacLeod, R. J., Kifor, O., Chattopadhyay, N., and Brown E. M. (2001) *J. Biol. Chem.* **276,** 34880–34887
63. Enz, R. (2002) *FEBS Lett.* **514,** 184–188
64. Onoprishvili, I., Andria, M. L., Kramer, H. K., Ancevska-Taneva, N., Hiller, J. M., and Simon, E. J. (2003) *Mol. Pharmacol.* **64,** 1092–1100
65. Seck, T., Baron, R., and Horne, W. C. (2003) *J. Biol. Chem.* **278,** 10408–10416
66. Lin, R., Canfield, V., and Levenson, R. (2002) *Pharmacology* **66,** 173–181
67. Zhang, M., and Breitwieser, G. E. (2005) *J. Biol. Chem.* **280,** 11140–11146
68. Huang, C., Wu, Z., Hujer, K. M., and Miller, R. T. (2006) *FEBS Lett.* **580,** 1795–1800
69. Marti, A., Luo, Z., Cunningham, C., Ohta, Y., Hartwig, J., Stossel, T. P., Kyriakis, J. M., and Avruch, J. (1997) *J. Biol. Chem.* **272,** 2620–2628
70. Ohita, Y., Suzuki, N., Nakamura, S., Hartwig, J. H., and Stossel, T. P. (1999) *Proc. Natl. Acad. Sci. U. S. A.* **96,** 2122–2128